

Biomass Burning Aerosol Fluorescence Spectra

Jens Reichardt, Felix Lauermann, Oliver Behrendt

*Deutscher Wetterdienst
Meteorologisches Observatorium Lindenberg, Germany
jens.reichardt@dwd.de*

Measurements with the spectrometric fluorescence and Raman lidar RAMSES in June 2023 are used to illustrate the general characteristics of the fluorescence spectrum of biomass burning aerosol (BBA). The BBA spectrum is often layer-specific, quite Gaussian with a center wavelength in the range of about 500 to 550 nm, and tends to shift to longer wavelengths with height. Fluorescence and elastic optical properties of BBA are only weakly correlated.

1. Introduction

BBA and other aerosols are widely monitored with lidars, which are often sophisticated instruments such as multiwavelength Raman lidars. Up until recently, however, the focus of the observations has been mostly on the elastic-optical properties of the aerosols even though it was demonstrated that measurements of their inelastic optical properties (fluorescence) offer additional useful information [1]. But this seems to be changing because more and more research groups are adding fluorescence capabilities to their lidar instruments. Unfortunately, only discrete fluorescence detection channels are often integrated instead of a fluorescence spectrometer. Such a limited experimental extension is certainly valuable, as it permits the use of fluorescence as an aerosol tracer within clouds and a rough aerosol typing, but it is not sufficient for the study of aerosol fluorescence per se.

An exception is RAMSES, the spectrometric fluorescence and Raman lidar of the German Meteorological Service at its Lindenberg site, Germany. RAMSES has been measuring the elastic and spectrally resolved inelastic properties of clouds and aerosols since 2011 using a combination of 12 discrete receiver channels and by now three spectrometers [1-3]. Over the years, a data set of several hundred fluorescence spectra of atmospheric aerosol has been accumulated; expansion, processing and analysis are ongoing.

In the free troposphere over Lindenberg, BBA layers are the most frequently observed aerosol events. Some examples of BBA fluorescence spectra have already been published [4,5]. In

this contribution, two measurements from June 2023 will be used to explain the general characteristics of the BBA fluorescence spectrum.

2. Measurement Parameters

The experimental details of RAMSES and the data evaluation techniques used to obtain absolutely calibrated Raman and fluorescence spectra are well documented in the literature [1-3], therefore only the measurement parameter set necessary for understanding the BBA observations is listed here.

After calibration, a spectrum consisting of spectral fluorescence backscatter coefficients (β^{FL}) is available at each height. If profiles are to be presented, β^{FL} is averaged over certain wavelength intervals (mean SFLBC), and a corresponding false color is assigned ($\beta^{\text{FL}}_{\text{color}}$). We use four false colors (blue, cyan, green, and red) with wavelength ranges of 430-450, 455-535, 545-625, and 630-710 nm, respectively. Furthermore, λ_c (CWL) indicates the wavelength of the maximum of the fluorescence spectrum, whereas λ_b and λ_r denote the wavelengths of the spectrum half widths on the short- and long-wavelength shoulder of the maximum, respectively.

Aerosol elastic properties used in this study are the particle backscatter coefficient (β_{par} , PBC), the particle depolarization ratio (δ_{par} , PDR), and the particle lidar ratio (S_{par} , PLR). An important combination of inelastic and elastic aerosol properties is the spectral fluorescence capacity, which is defined as the ratio of β^{FL} to β_{par} [1]. In this study it is either presented as a false color average, or spectrally resolved.

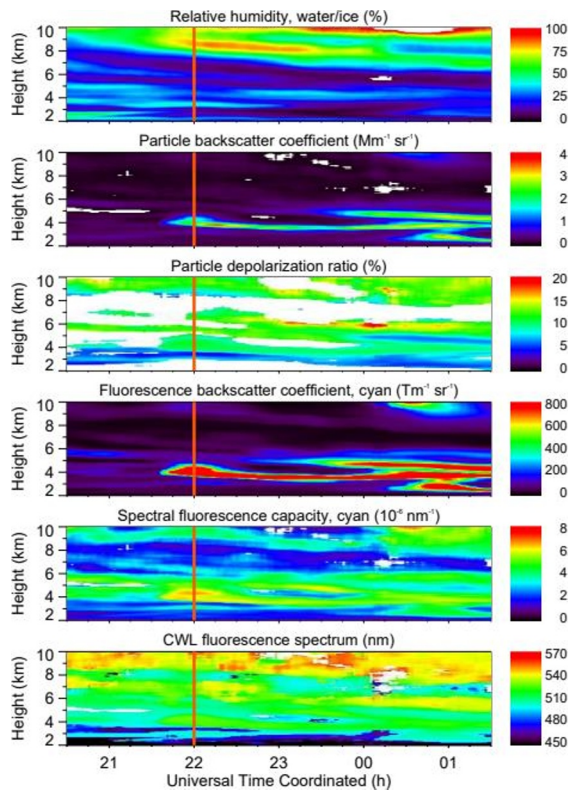


Figure 1. BBA measurement in the night of 1-2 June 2023. Profiles and fluorescence spectra measured at 22 UTC (time marked by vertical orange line) are analyzed in Figs. 3 and 5.

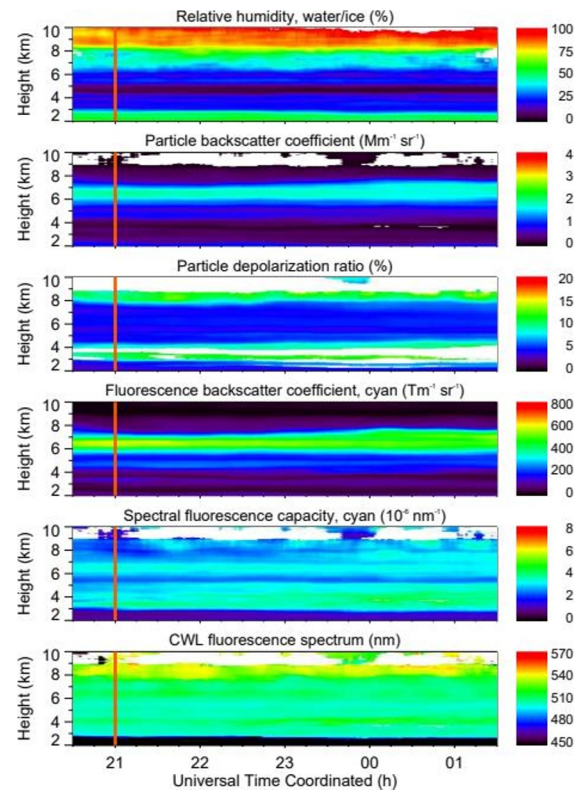


Figure 2. BBA measurement in the night of 4-5 June 2023. Profiles and fluorescence spectra measured at 21 UTC are presented in Figs. 4 and 6.

Relative humidity (RH) is obtained from the RAMSES measurement of water vapor mixing ratio and, in this study, from interpolated temperature (T) data from the six-hourly radiosonde launches on site.

3. BBA Measurement Examples

Figure 1 presents the RAMSES measurement in the night of 1-2 June 2023. BBA is present in the entire free troposphere, especially below 6 km, where a dominant BBA layer develops starting at 21:40 UTC. Except for the humid layer near the tropopause, RH is low, and the PDR values of the BBA are comparatively high at all heights. Fluorescence backscatter coefficient (cyan false color) and PBC are correlated, which explains the relatively homogeneous mean spectral capacity. CWL shows a clear structure which corresponds with the BBA filaments.

During the night of 4-5 June 2023, the BBA field is more homogeneous and horizontally stratified (Fig. 2). As before, the atmosphere is

dry within the aerosol layer and cloud-free. In contrast, however, BBA PDR, fluorescence backscatter coefficient, spectral fluorescence capacity, and CWL are all lower.

The differences are particularly evident when the profiles measured on 1 June 2023 at 22 UTC and 4 June 2023 at 21 UTC are compared (Figs. 3 and 4). The main BBA layers exhibit opposing trends in PDR (11 % vs. 4 %) and PLR (< 40 sr vs. 60 sr), indicating a different composition, shape or size distribution of the carrier substances of the fluorophores.

The mean SFLBC curves appear to be similar at first sight, but on closer inspection they reveal slightly different trends. As a result, the wavelengths characterizing the shape of the BBA fluorescence spectrum (λ_b , λ_c , and λ_r) generally increase with height (the red shift is slightly faster on 1 June 2023 than on 4 June 2023), while there may also be a layer-specific blue shift (only on 1 June 2023, e.g., around 5 km).

Figure 5 shows BBA fluorescence spectra for selected heights measured on 1 June 2023 at

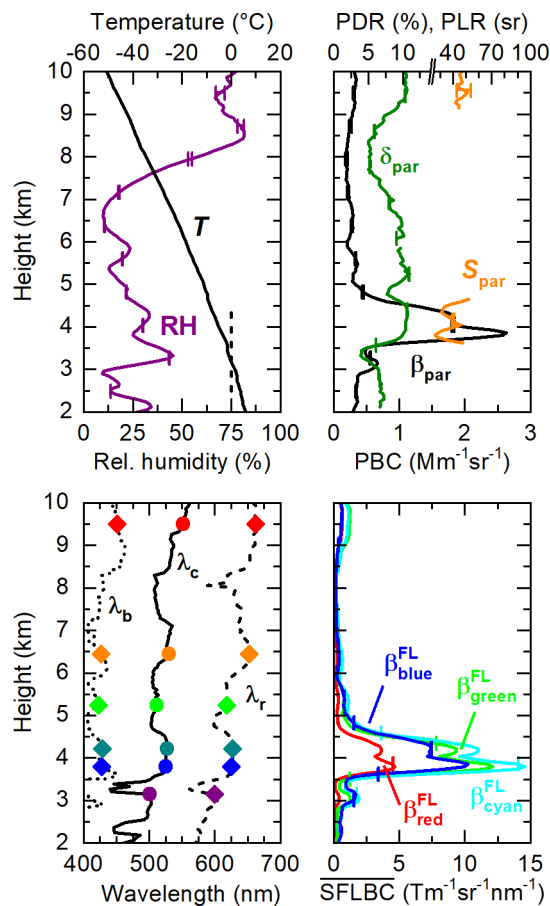


Figure 3. Profile measurement of the BBA layer at 22 UTC on 1 June 2023. The vertical dashed line marks the freezing level. Colored symbols indicate heights for which the fluorescence spectra are presented in Fig. 5.

22 UTC. Three different forms of presentation were chosen. Firstly, the β^{FL} spectrum, which is the direct product of the processing and calibration of the spectrometer data. It shows the absolute β^{FL} values as measured at a certain height, so it depends, among other factors, on the aerosol load. This dependence is approximately removed when, secondly, the spectrum of fluorescence capacity is considered. The convergence of the curves suggests that the normalization to PBC can help the interpretation of the spectra. Thirdly, the capacity spectra are displayed in relation to a reference capacity spectrum. These capacity-ratio spectra permit an understanding of the dynamics of the BBA spectrum: a horizontal offset means that only the fluorescence capacity but not the shape of the BBA spectrum has changed with respect to the reference spectrum; in contrast, a positive gradient indicates a red shift and a negative gradient a blue shift of the

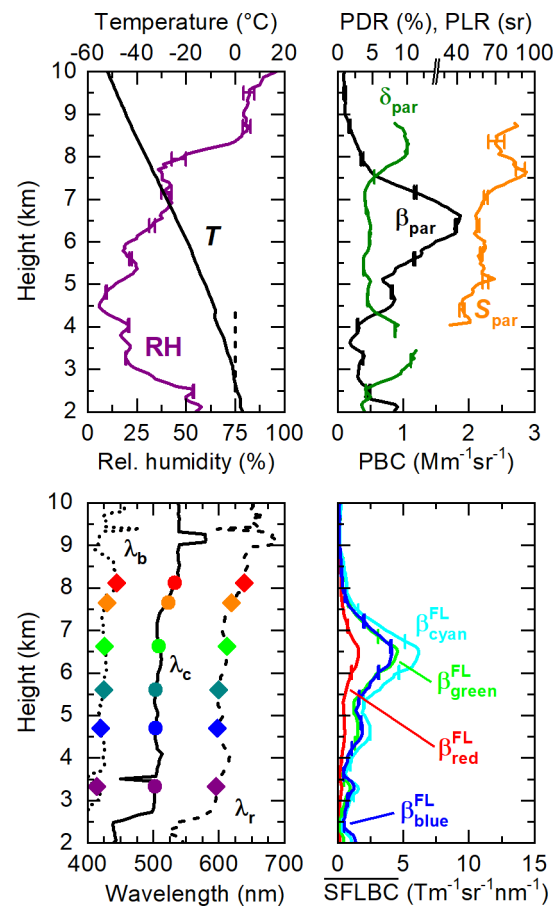


Figure 4. Profile measurement of the BBA layer at 21 UTC on 4 June 2023. Colored symbols indicate heights for which the fluorescence spectra are presented in Fig. 6.

spectrum under consideration.

The BBA spectra in Fig. 5 are spectrally broad, without distinctive features and have their maximum between 500 and 550 nm (altitudes and CWL are indicated in the legend; the reference spectrum is marked with an asterisk). The shape is approximately Gaussian. In fact, curve fits show that the agreement improves with height.

With regard to the reference spectrum at 5.2 km, all fluorescence spectra at and above 3.8 km are red-shifted, particularly strongly at 9.5 km (the gradient of the fluorescence capacity ratio is maximum). On 4 June 2023, the spectral properties are different (Fig. 6). CWL is mostly at shorter wavelengths, and the red shift with height is slower. Furthermore, the fluorescence capacity is diminished compared to the first measurement example. This also applies to its variability, and the dynamics is higher at shorter than at longer wavelengths.

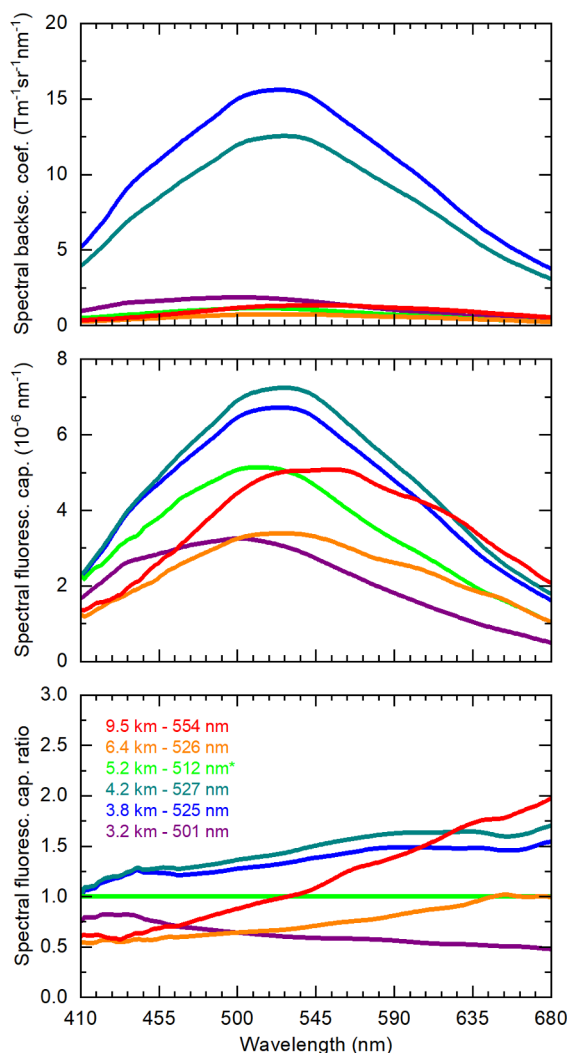


Figure 5. Spectral measurements of the BBA layer at 22 UTC on 1 June 2023.

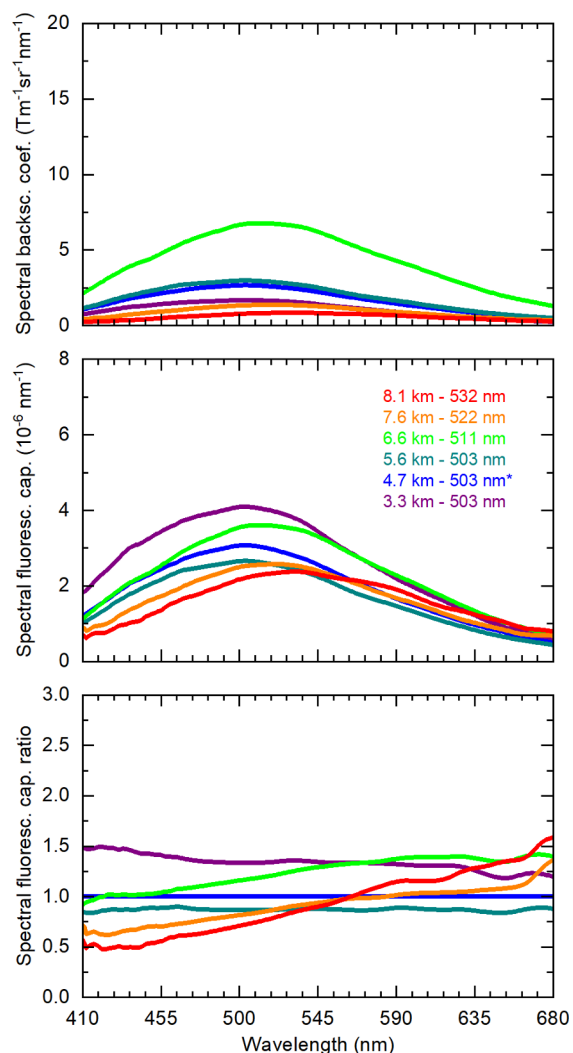


Figure 6. Spectral measurements of the BBA layer at 21 UTC on 4 June 2023.

In summary, our BBA examples illustrate how diverse aerosol events can be, but also how subtle the differences are. To exploit the rich information content aerosol fluorescence offers, spectral measurements are definitely required, a single or a couple of discrete detection channels is not sufficient. Finally, an interesting question is whether it is possible to relate the observed spectral differences to specific burning events. Our trajectory analyses show that on 1 June 2023 the BBA source were wildfires in northern Alberta, Canada, where mixed forests prevail while three days later the origin was further to the east in Saskatchewan with predominantly coniferous forests. Work on this interesting field is ongoing.

[1] J. Reichardt, "Cloud and aerosol spectroscopy with Raman lidar," *J. Atmos. Ocean. Tech.* **31**, 1946-1963 (2014).

[2] J. Reichardt, U. Wandinger, V. Klein, I. Mattis, B. Hilber and R. Begbie, "RAMSES: German Meteorological Service autonomous Raman lidar for water vapor, temperature, aerosol, and cloud measurements," *Appl. Opt.* **51**, 8111-8131 (2012).

[3] J. Reichardt, O. Behrendt and F. Lauer mann, "Spectrometric fluorescence and Raman lidar: absolute calibration of aerosol fluorescence spectra and fluorescence correction of humidity measurements," *Atmos. Meas. Tech.* **16**, 1-13 (2023).

[4] J. Reichardt, R. Leinweber and A. Schweb e, "Fluorescing aerosols and clouds: investigations of co-existence," *EPJ Web of Conferences* **176**, 05010 (2018).

[5] J. Reichardt, F. Lauer mann and O. Behrendt, "Aerosol studies with spectrometric fluorescence and Raman lidar," in *Proceedings of the 30th International Laser Radar Conference*, J. T. Sullivan, and Coeditors (Springer International Publishing, Cham, 2023), pp. 279-285.